Electronic Supplementary Material (ESI) for ChemComm.


# Tetrameric Psuedo-Peptide Receptors with Allosteric Properties

*Mee-Kyung Chung,[a] Stephen J. Lee,[b] Marcey L. Waters[a]* and Michel R. Gagné[a]**

[a]Department of Chemistry, University of North Carolina at Chapel Hill, Chapel Hill, NC 27599-3290, USA. [b]US Army Research Office, P.O. Box 12211, Research Triangle Park, NC 27709, USA

## *Supporting Information*

*Contents*

## Experimental Details

### General Methods.

Chemicals were purchased from Aldrich, Fisher Scientific and Chem-Impex International, Inc. and used as received. $^{1}H$ and $^{13}C$ NMR spectra of monomers and $^{1}H$, $^{13}C$, and HSQC NMR spectra of tetramers were recorded on a Bruker DRX 500 spectrometer or a Bruker 600 Cryoprobe spectrometer and processed using TOPSPIN Bruker NMR software (V. 3.0). High resolution mass spectra were obtained on an Agilent Accurate LC-TOF Mass Spectrometer (Agilent Series 6220) operating in positive ion mode with electrospray ionization source (fragmentor = 170V). The data were analyzed using Agilent MassHunter Workstation Software, Qualitative Analysis (V. B.02.00). HPLC analysis was performed on a Hewlett-Packard Series 1100 instrument, using a Halo-C18 column (4.6 x 150 mm, 2.7 μm) with gradient elution (methanol/water) at a flow rate of 0.45 mL/min and at 55 ºC. The injection volume for a 5 mM Dynamic combinatorial library (DCL) reaction was typically 3.5 μL. UV absorbance chromatograms were recorded at wavelengths of 220 nm and 289 nm. The data were analyzed using Agilent Chemstation. The isolation of tetramers was performed on a modified semi-preparative HPLC (Agilent Series 1200 LC instrument), using an Agilent Zorbax Eclipse XDB-C18 PrepHT Cartridge column (21.2 x 250 mm, 7 μm) with isocratic methanol/water elution (no additive) at a flow rate of 9 mL/min and at 55 ºC. The eluent was monitored by UV absorbance chromatogram at a wavelength of 289 nm and the corresponding tetramers were collected with a fraction collector. X-ray crystallographic analyses of tetramers **1a** and **1b** were performed on a Bruker-AXS SMART APEX-II system equipped with a graphite monochromator: please contact Dr. Peter S. White (pwhite@email.unc.edu) for correspondence regarding X-ray analyses.

### Synthesis of monomers

D-Pro-Aib and D-Pro-α-Me-L-Phe were prepared using previously reported methods. [1] A coupling reaction using HBTU, HOBt and $Et_3N$ in DMF from D-Pro precursor and methyl esters of Aib or α-Me-L-Phe, followed by the subsequent treatment with hydrazine monohydrate in methanol at ambient temperature resulted the corresponding D-Pro-Aib (previously reported) and D-Pro-α-Me-L-Phe (New) monomers. The total isolated yields for the two step reactions were 43-48%.

(i) *Physical data of D-Pro-α-Me-L-Phe* $^{1}H$ NMR (600.1 MHz, $CDCl_3$, 23 ºC): $\delta$ = 8.36 (s, 1H), 7.48 (d, $J$ = 8.2 Hz, 2H), 7.41 (d, $J$ = 8.3 Hz, 2H), 7.30 – 7.27 (m, 3H), 7.16 (d, $J$ = 8.1 Hz, 2H), 6.58 (s, 1H), 5.40 (s, 1H), 4.42 (dd, $J$ = 7.9, 5.6 Hz, 1H), 3.85 (d, $J$ = 4.2 Hz, 1H), 3.54 – 3.46 (m, 3H), 3.32 (s, 6H), 2.98 (d, $J$ = 13.7 Hz, 1H), 2.25 (m, 1H), 2.14 (m, 1H), 2.06 (m, 1H), 1.86 (m, 1H), 1.59 (s, 3H). $^{13}C$ NMR (150.9 MHz, $CDCl_3$, 23 ºC): $\delta$ = 173.6, 171.3, 170.9, 140.5, 135.6, 135.4, 130.3, 128.5, 127.2, 127.1, 126.7, 102.3, 61.5, 60.1, 52.7, 50.5, 43.0, 28.2, 25.5, 23.7. HRMS (ESI): calcd for $C_{25}H_{33}N_4O_5^+$ $[M+H]^+$ 469.2445, found 469.2456.

[1] Voshell, S. M.; Lee, S. J.; Gagné, M. R. *J. Am. Chem. Soc.* **2006**, *128*, 12422-12423.

**Synthesis of tetramers and generation of 1a and 1b crystals for X-ray analysis**

Several 5 mM DCL solutions were prepared on a 20 mL scale. Each was prepared by dissolving the D-Pro-Aib and D-Pro-α-Me-L-Phe (100.0 μmol) in 100% acetonitrile (20 mL) and subsequently adding trifluoroacetic acid (50 equiv, 5000 μmol) and the guest (-)-cytidine (10 equiv, 1000 μmol). The solutions were allowed to sit for several days until a steady state was reached (typically 7-10 days) prior to LC analyses. Once they reached their steady state, triethylamine (50 equiv, 5000 μmol) was added to neutralize the acid. The solutions were combined and the volatiles were removed in vacuo. The minimum amount of 80% methanol/chloroform solution was added to the resulting mixture and then filtered. This solution was eluted on the semi-preparative HPLC with various methanol/water isocratic solutions to isolate the tetramers. Recrystallization of **1a** from methanol/water by slow evaporization at RT for a few weeks offered crystals suitable for the X-ray analysis. For the tetramer **1b**, recrystallization from methanol/chloroform by slow evaporization at RT resulted in crystals suitable for the X-ray analysis.

**Physical data of tetramer 1a and 1b: both are new compounds**

(ii) Physical data of **1a** $^{1}$H NMR (600.1 MHz, MeCN-$d_3$, 23 $^{o}$C): $\delta$ = 10.69 (s, 1H), 7.94 (s, 1H), 7.40 (s, 1H), 7.37 (d, $J$ = 8.2 Hz, 2H), 6.90 (d, $J$ = 7.9 Hz, 2H), 4.34 (t, $J$ = 8.1 Hz, 1H), 3.75 (m, 1H), 3.38 (m, 1H), 2.12 – 2.03 (m, 3H), 1.77 (m, 1H), 1.53 (s, 3H), 1.48 (s, 3H). $^{1}$H NMR (600.1 MHz, MeOH-$d_4$, 23 $^{o}$C): $\delta$ = 7.93 (s, 1H), 7.45 (d, $J$ = 8.0 Hz, 2H), 6.99 (d, $J$ = 7.0 Hz, 2H), 4.47 (t, $J$ = 8.4 Hz, 1H), 3.90 (m, 1H), 3.42 (m, 1H), 2.20 – 2.13 (m, 3H), 1.79 (m, 1H), 1.60 (s, 3H), 1.55 (s, 3H). $^{13}$C NMR (150.9 MHz, MeOH-$d_4$, 23 $^{o}$C): $\delta$ = 174.7, 174.6, 171.0, 148.3, 138.5, 138.2, 129.1, 128.1, 63.2, 57.9, 51.9, 30.0, 27.8, 27.5, 24.0. HRMS (ESI): calcd for $C_{68}H_{81}N_{16}O_{12}^{+}$ $[M+H]^{+}$ 1313.6214, found 1313.6215.

(iii) Physical data of **1b** $^{1}$H NMR (600.1 MHz, MeCN-$d_3$, 23 $^{o}$C): $\delta$ = 10.67 (s, 1H), 8.17 (s, 1H), 7.54 (d, $J$ = 7.9 Hz, 2H), 7.38 – 7.27 (m, 5H), 7.21 (d, $J$ = 13.5 Hz, 1H), 6.90 (s, 1H), 4.30 (t, $J$ = 7.9 Hz, 1H), 3.67 (m, 1H), 3.42 (m, 2H), 3.10 (d, $J$ = 13.5 Hz, 1H), 2.28 (m, 1H), 2.01 (m, 1H), 1.89 (m, 1H), 1.81 (m, 1H), 1.40 (m, 3H). $^{1}$H NMR (600.1 MHz, 10%MeCN-$d_3$/$CD_2Cl_2$, 23 $^{o}$C): $\delta$ = 10.59 (s, 1H), 7.94 (s, 1H), 7.40 – 7.21 (m, 9H), 6.56 (s, 1H), 4.24 (m, 1H), 3.68 (m, 1H), 3.40 (m, 1H), 3.30 (d, $J$ = 13.4 Hz, 1H), 2.20 (m, 1H), 2.08 (m, 1H), 1.88 (m, 1H), 1.72 (m, 1H), 1.51 (m, 3H). $^{13}$C NMR (150.9 MHz, 10% MeCN-$d_3$/$CD_2Cl_2$, 23 $^{o}$C): $\delta$ = 172.0, 170.4, 146.6, 137.2, 136.8, 135.8, 131.0, 128.8, 128.0, 127.6, 127.1, 63.0, 60.4, 51.1, 44.5, 29.4, 26.3, 22.9. HRMS (ESI): calcd for $C_{92}H_{97}N_{16}O_{12}^{+}$ $[M+H]^{+}$ 1617.7466, found 167.7425.

**Crystal data of tetramer 1a and 1b**

(i) Crystal data of **1a**: Identification code **X1007002**, ($C_{68}H_{80}N_{16}O_{12}$), M = 1313.48 g/mol, crystal dimensions 0.414 x 0.198 x 0.076 mm$^3$, orthorhombic, space group $P2_12_12_1$, cell parameters a = 22.2194(6) Å, b = 26.8073(8) Å, c = 30.7909(8) Å, α = 90º, β = 90º, γ = 90º, V = 18340.4(9) Å$^3$, T = 100.0 K, Z = 8, $\rho_{calcd}$ = 0.951 g cm$^{-3}$, μ (MoKα) = 0.549 mm$^{-1}$. 40540 reflections were measured (1.65° ≤ 2Θ ≤ 126.06°), 13600 unique ($R_{int}$ = 0.0996) which were used all calculations. Index ranges are -24≤h≤25, 0≤k≤29 and 0≤l≤35. Using Olex2, the structure was solved with the XM structure program using Dual Space and refined with the XL refinement package using Least Squares minimization. The

final $R_1$ = 0.0692, $wR_2$ = 0.1673 for I>2σ(I) and $R_1$ = 0.1005, $wR_2$ = 0.1830 for all data. GOF = 0.868, max/min residual density 0.248/-0.254 $e^{-}Å^{-3}$.

(ii) Crystal data of **1b**: Identification code **X1204022** (**MKC-5073**), $C_{98}H_{120}N_{16}O_{18}$, M = 1810.09, crystal dimensions 0.367 x 0.232 x 0.216 mm, tetragonal, space group $P4_32_12$, cell parameters a = 15.4204(2) Å, b = 15.4204(2) Å, c = 43.9852(6) Å, α = 90.00º, β = 90.00º, γ = 90.00º, V = 10459.2(3) Å, T = 100.0 K, Z = 4, $\rho_{calcd}$ = 1.150 mg $mm^{-3}$, μ = 0.655 $mm^{-1}$, radiation CuKα, λ = 1.54178 Å. 71295 reflections were measured (6.074° ≤ 2Θ ≤ 133.198°), 9227 unique ($R_{int}$ = 0.0431, $R_{sigma}$ = 0.0234) were used in all calculations. Index ranges are -18≤h≤17, -18≤k≤18 and -52≤l≤52. Using Olex2, the structure was solved with the XM structure program using Dual Space and refined with the XL refinement package using Least Squares minimization. The final $R_1$ = 0.0663, $wR_2$ = 0.1836 for I>2σ(I) and $R_1$ = 0.0717, $wR_2$ = 0.1884 for all data, GOF = 1.058; max/min residual density 0.56/-0.31 $e^{-}Å^{-3}$. Flack parameter = 0.10(8).

**SI Table 1.** Relative yields (%) and amplification factors (A.F.) of tetramers **1a** and **1b** obtained from their corresponding dynamic combinatorial libraries (DCLs).

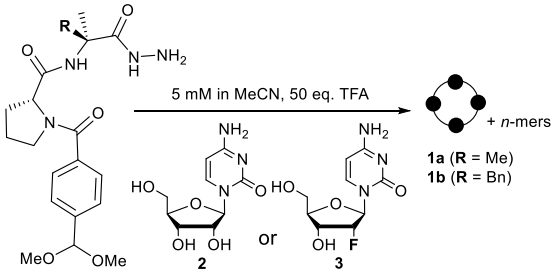


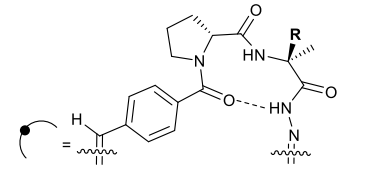


| Tetramer | Guest | Yield (%)[a] | A. F.[b] |
|---|---|---|---|
| **1a** | **2** | 86 | 1.5 |
| | **3** | 76 | 1.4 |
| **1b** | **2** | 73 | 3.3 |
| | **3** | 63 | 2.9 |

[a]Relative yields obtained from HPLC-UV (289 nm) traces of DCLs formed from D-Pro-Aib or D-Pro-α-Me-L-Phe. [b]The amounts of tetramers **1a** and **1b** in the corresponding untemplated DCLs were 56 and 22 % yields, respectively.

**SI Table 2.** β-turn types and dihedral angles in **1a** and **1b**.

| | | **1a** | | **1b** | |
|---|---|---|---|---|---|
| | | angles | type | angles | type |
| β-1 | $\Phi_{i+1}$ | 61.2 | II′[a] | 60.0 | II′[a] |
| | $\Psi_{i+1}$ | -145.3 | | -128.4 | |
| | $\Phi_{i+2}$ | -59.1 | | -55.8 | |
| | $\Psi_{i+2}$ | -31.3 | | -31.4 | |
| β-2 | $\Phi_{i+1}$ | 59.2 | Deviated II′[b] | 61.2 | II′[a] |
| | $\Psi_{i+1}$ | -168.2 | | -132.6 | |
| | $\Phi_{i+2}$ | -49.2 | | -61,4 | |
| | $\Psi_{i+2}$ | -53.6 | | -17.8 | |
| β-3 | $\Phi_{i+1}$ | 50.0 | II′[a] | 60.0 | II′[a,c] |
| | $\Psi_{i+1}$ | -136.3 | | -128.4 | |
| | $\Phi_{i+2}$ | -48.8 | | -55.8 | |
| | $\Psi_{i+2}$ | -38.3 | | -31.5 | |
| β-4 | $\Phi_{i+1}$ | 60.8 | II′[a] | 61.2 | II′[a,d] |
| | $\Psi_{i+1}$ | -147.9 | | -132.6 | |
| | $\Phi_{i+2}$ | -63.4 | | -61.4 | |
| | $\Psi_{i+2}$ | -15.1 | | -17.8 | |

[a]Using normal cutoffs of 40º for deviation from standard angles, with one angle allowed deviated by 50º, these β-turns can be classified as type II′ (standard mean dihedral angles: $\Phi_{i+1}$, 60º; $\Psi_{i+1}$, -126º; $\Phi_{i+2}$, -91º; $\Psi_{i+2}$, 1º). See the ref.: Hutchinson, E. G.; Thornton, J. M. *Protein Sci.* **1994**, *3*, 2207-2216. [b]Using the same cutoffs (normal cutoffs of 40º for deviation from standard angles, with one angle allowed extensively deviated by 50º), this β-turn cannot be classified as type II′. However, this β-turn can be classified as type II′ when normal cutoffs of 45º for deviation from standard angles are employed: that is, deviated type II′. [c]By symmetry, dihedral angles and the turn type are the same as the β-1 turn. [d]By symmetry, dihedral angles and turn type are the same as the β-2 turn.

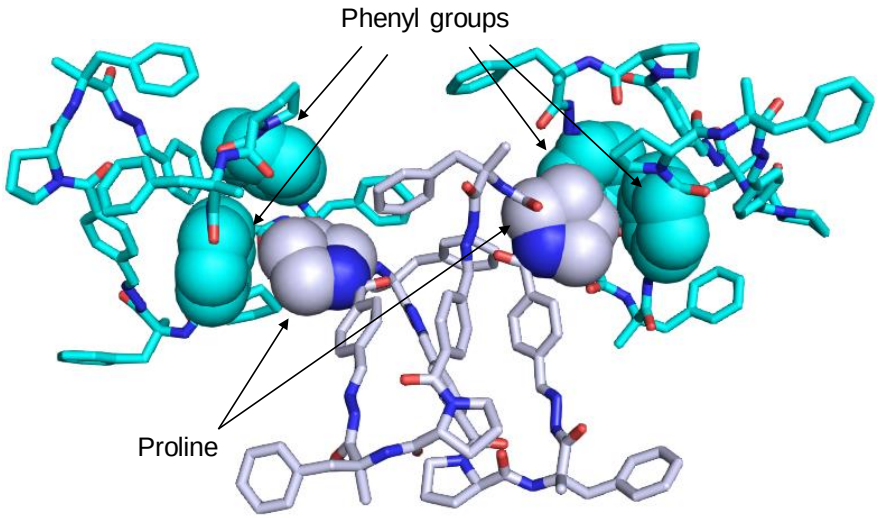


**SI Figure 1.** Packing diagram of tetramer **1b** showing how the prolines (space-filled shapes) of one molecule (gray) intrude into the binding cavity of another. Phenyl groups of the binding cavity are shown as space-filled shapes.

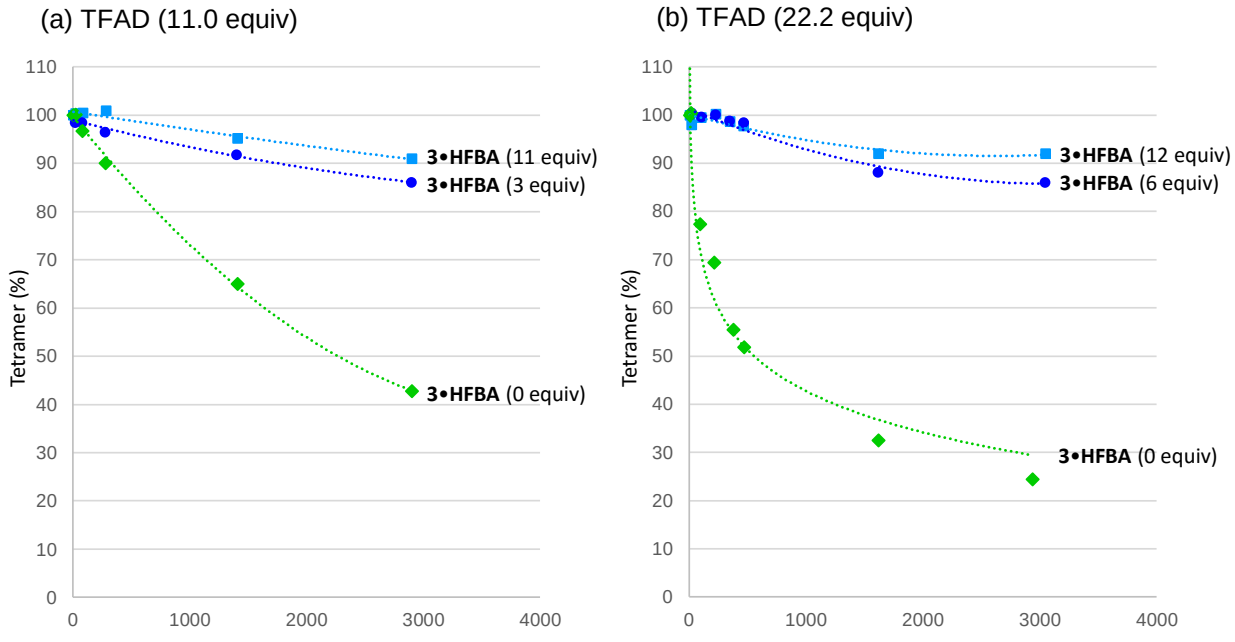


**SI Figure 2.** Plot of the contents **1b** in solution vs time as a function of added **3•HFBA** under acidic conditions: (a) 11.0 and (b) 22.2 equiv of TFAD addition.

(a) **1a** and **3•HFBA**

(i) 1:1 host-guest scenario

$$H + G \rightleftharpoons H\text{-}G$$

$$K_{eq} = \frac{[H\text{-}G]}{[H][G]} \qquad [H\text{-}G] = K_{eq}[H][G]$$

$$K_D = \frac{[H][G]}{[H\text{-}G]} \qquad [H][G] = K_D[H\text{-}G]$$

[H-G] and [H][G]: linear relationship.

(ii) 1:2 host-guest scenario

$$H + 2G \rightleftharpoons H\text{-}G_2$$

$$K_{eq} = \frac{[H\text{-}G_2]}{[H][G]^2} \qquad [H\text{-}G_2] = K_{eq}[H][G]^2$$

$$K_D = \frac{[H][G]^2}{[H\text{-}G_2]} \qquad [H][G]^2 = K_D[H\text{-}G_2]$$

$[H\text{-}G_2]$ and $[H][G]^2$: linear relationship.

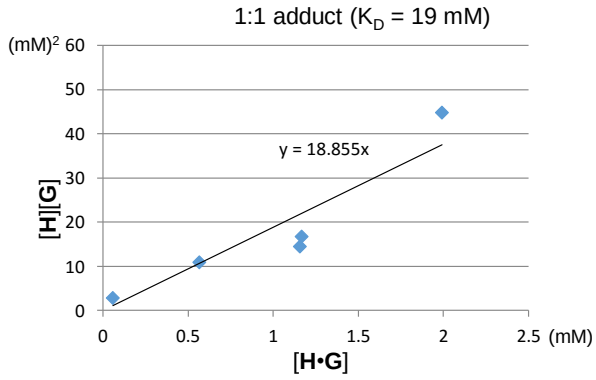


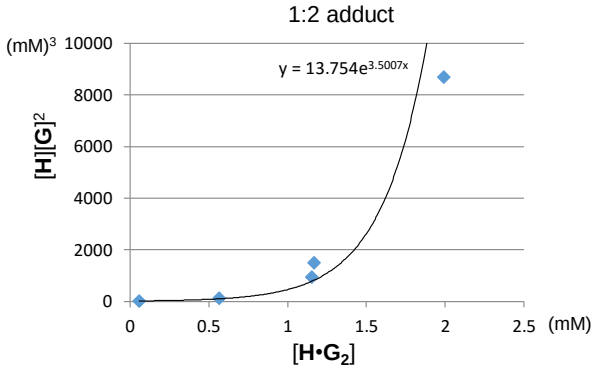


(b) **1b** and **3•HFBA**

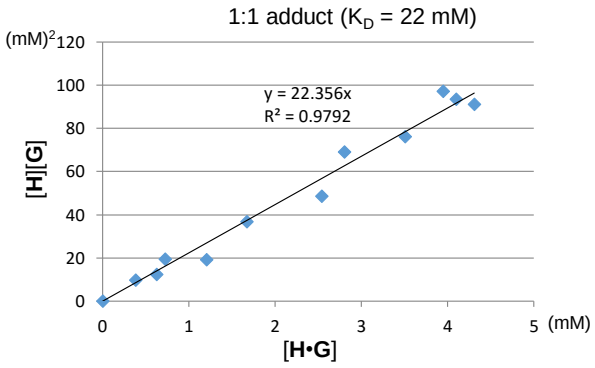


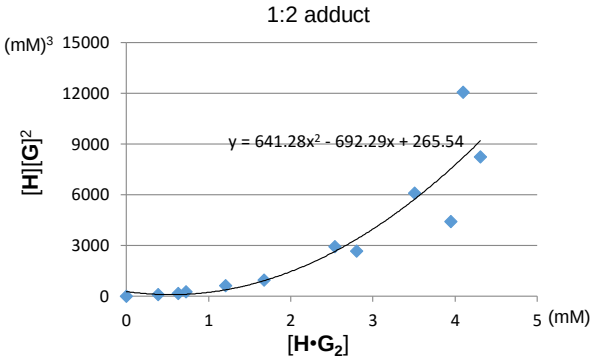


Since only [H][G] and [H-G] display linear relationships for **1** and **3•HFBA**, the binding is consistent with a 1:1 stiochiometry: $K_D$ = 19 and 22 mM for **1a** and **1b**, respectively.

**SI Figure 3.** Dissociation constant determination for the binding of tetramers **1** and various equivalents of **3•HFBA** at room temperature. The data were obtained from the ratio of the host-guest methyl and free host methyl in $^1$H NMR spectra of the mixture of tetramers **1** and **3•HFBA** (100% MeCN-$d_3$).

(a) **1a** and **3•HFBA**

(i) 1:1 host-guest scenario

$$H + G \rightleftharpoons H\text{-}G$$

$$K_{eq} = \frac{[H\text{-}G]}{[H][G]} \qquad [H\text{-}G] = K_{eq}[H][G]$$

$$K_D = \frac{[H][G]}{[H\text{-}G]} \qquad [H][G] = K_D[H\text{-}G]$$

[H-G] and [H][G]: linear relationship.

(ii) 1:2 host-guest scenario

$$H + 2G \rightleftharpoons H\text{-}G_2$$

$$K_{eq} = \frac{[H\text{-}G_2]}{[H][G]^2} \qquad [H\text{-}G_2] = K_{eq}[H][G]^2$$

$$K_D = \frac{[H][G]^2}{[H\text{-}G_2]} \qquad [H][G]^2 = K_D[H\text{-}G_2]$$

$[H\text{-}G_2]$ and $[H][G]^2$: linear relationship.

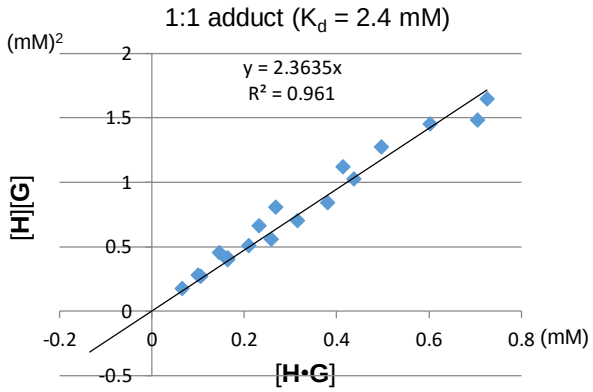


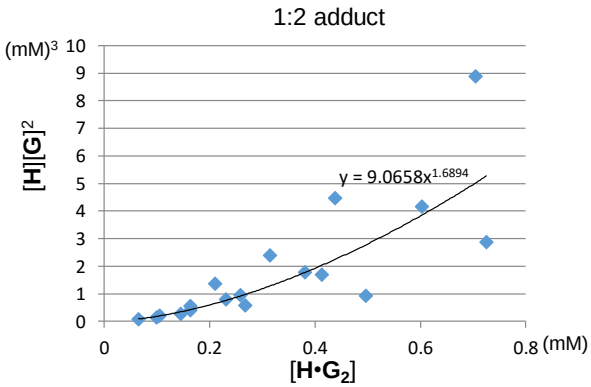


(b) **1b** and **3•HFBA**

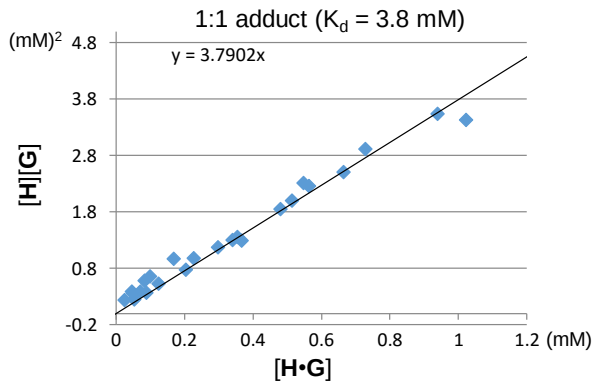


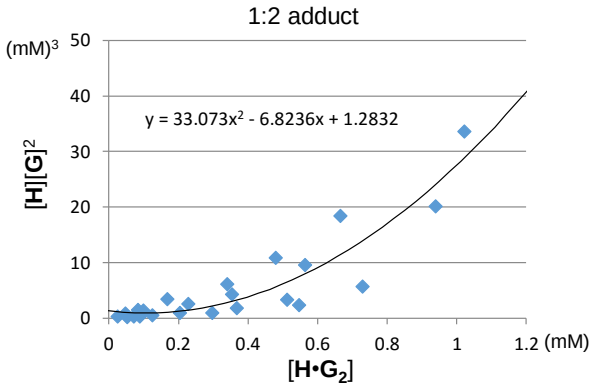


Since only [H][G] and [H-G] display linear relationships for **1** and **3•HFBA**, the binding is consistent with a 1:1 binding stoichiometry: $K_D$ = 2.4 and 3.8 mM for **1a** and **1b**, respectively.

**SI Figure 4.** Dissociation constant determination for the binding of tetramers **1** and various equivalents of **3•HFBA** under acidic condition at room temperature. The data were obtained from the ratio of the host-guest methyl and free host methyl in $^1$H NMR spectra of the mixture of tetramers **1**, **3•HFBA**, and TFAD (11.0 equiv/host) (100% MeCN-$d_3$).

(i) 1:1 host-guest scenario

$$H + G \rightleftharpoons H\text{-}G$$

$$K_{eq} = \frac{[H\text{-}G]}{[H][G]} \qquad [H\text{-}G] = K_{eq}[H][G]$$

$$K_D = \frac{[H][G]}{[H\text{-}G]} \qquad [H][G] = K_D[H\text{-}G]$$

[H-G] and [H][G]: linear relationship.

(ii) 1:2 host-guest scenario

$$H + 2G \rightleftharpoons H\text{-}G_2$$

$$K_{eq} = \frac{[H\text{-}G_2]}{[H][G]^2} \qquad [H\text{-}G_2] = K_{eq}[H][G]^2$$

$$K_D = \frac{[H][G]^2}{[H\text{-}G_2]} \qquad [H][G]^2 = K_D[H\text{-}G_2]$$

$[H\text{-}G_2]$ and $[H][G]^2$: linear relationship.

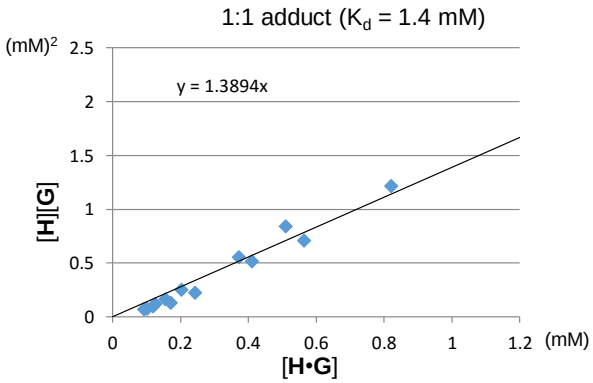


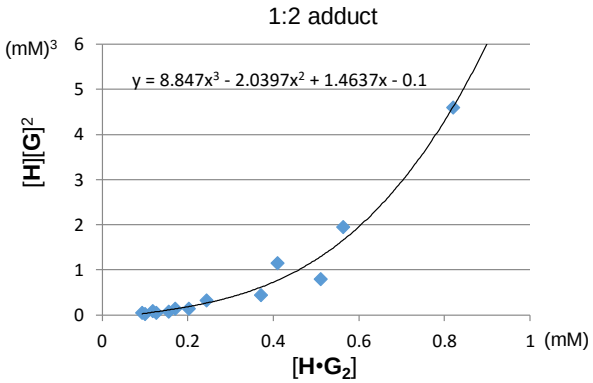


Since only [H][G] and [H-G] display linear relationships for **1b** and **3•HFBA**, the binding is consistent with a 1:1 soichiometry: $K_D$ = 1.4 mM for **1b**.

**SI Figure 5.** Dissociation constant determination for the binding of tetramer **1b** and various equivalents of **3•HFBA** under acidic condition at room temperature (10% MeCN-$d_3$/$CD_2Cl_2$). The data were obtained from the ratio of the host-guest methyl and free host methyl in $^1$H NMR spectra of the mixture of tetramers **1**, **3•HFBA**, and TFAD (11.0 equiv/host).

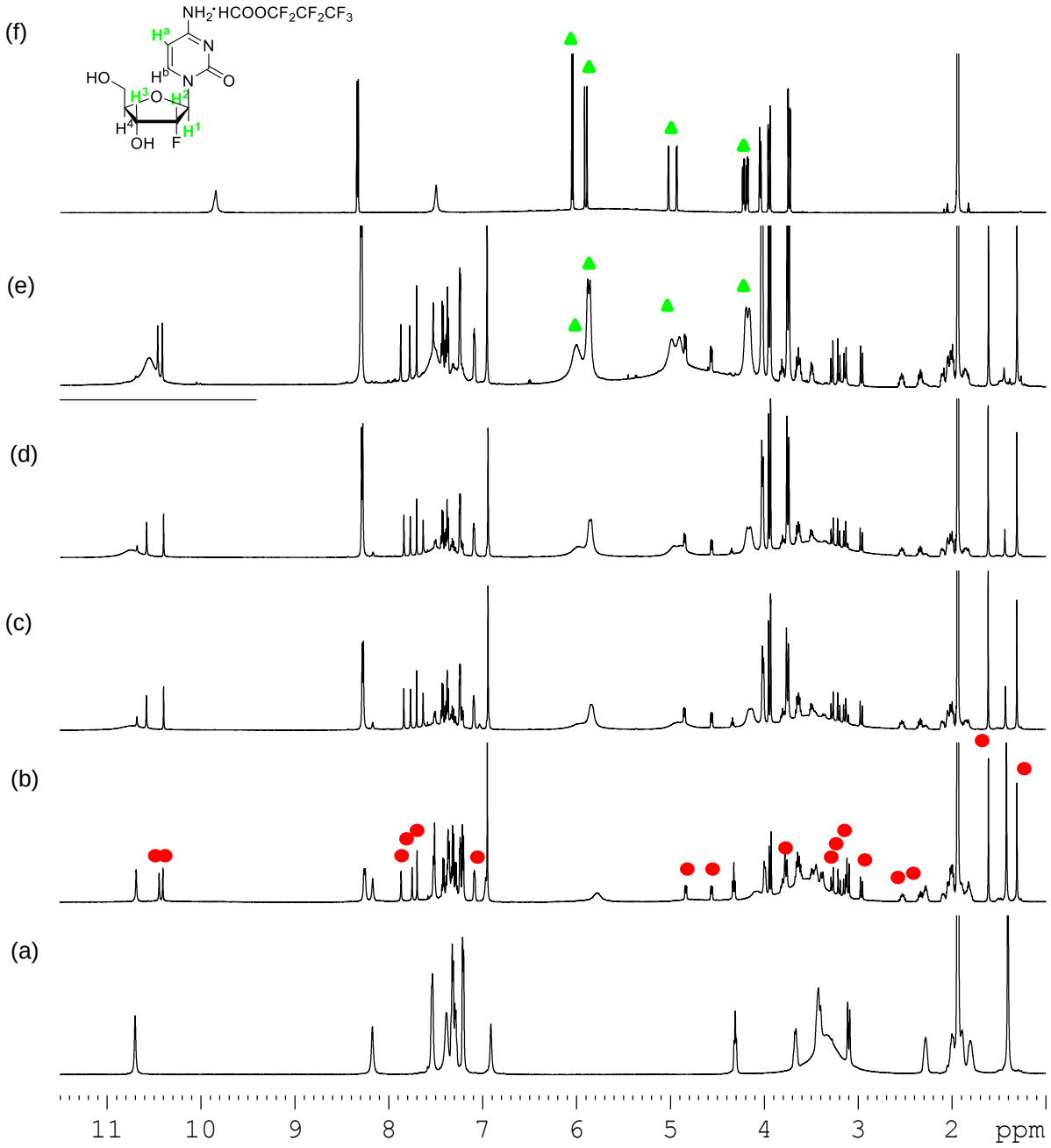


▲: $H^1$, $H^2$, $H^3$, and $H^a$ signals of **3•HFBA** in (f). ●: Newly generated peaks after the addition of **3•HFBA** to the mixture of **1b** and TFAD in 10%MeCN-$d_3$/$CD_2Cl_2$, which are corresponding to Host-Guest adduct signals.

**SI Figure 6.** Stacked $^1$H NMR spectra of the mixtures of **1b** (1.8 mM), TFAD (19.8 mM = 11.0 equiv), and various equivalents of **3•HFBA** in 10% MeCN-$d_3$/$CD_2Cl_2$ at room temperature ((a) – (e)). The equivalents of **3•HFBA** are (a) 0.0 equiv, (b) 3.1 equiv, (c) 10.8 equiv, (d) 13.2 equiv and (e) 20.1 equiv. (f) $^1$H NMR spectrum of **3•HFBA** (4.3 mM) and TFAD (20.8 mM) in 10%MeCN-$d_3$/$CD_2Cl_2$ at room temperature.

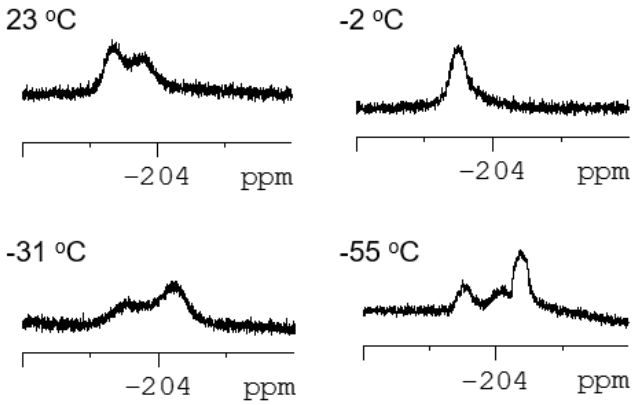


**SI Figure 7.** Variable temperature $^{19}F$ NMR spectra from the combination of 2.5 equiv of **3•HFBA** (2'-F) and **1b** (2.7 mM) in 10% MeCN-$d_3$/$CD_2Cl_2$; and TFAD (12 equiv). The upfield resonance at -55 °C corresponds to free **3•HFBA**.

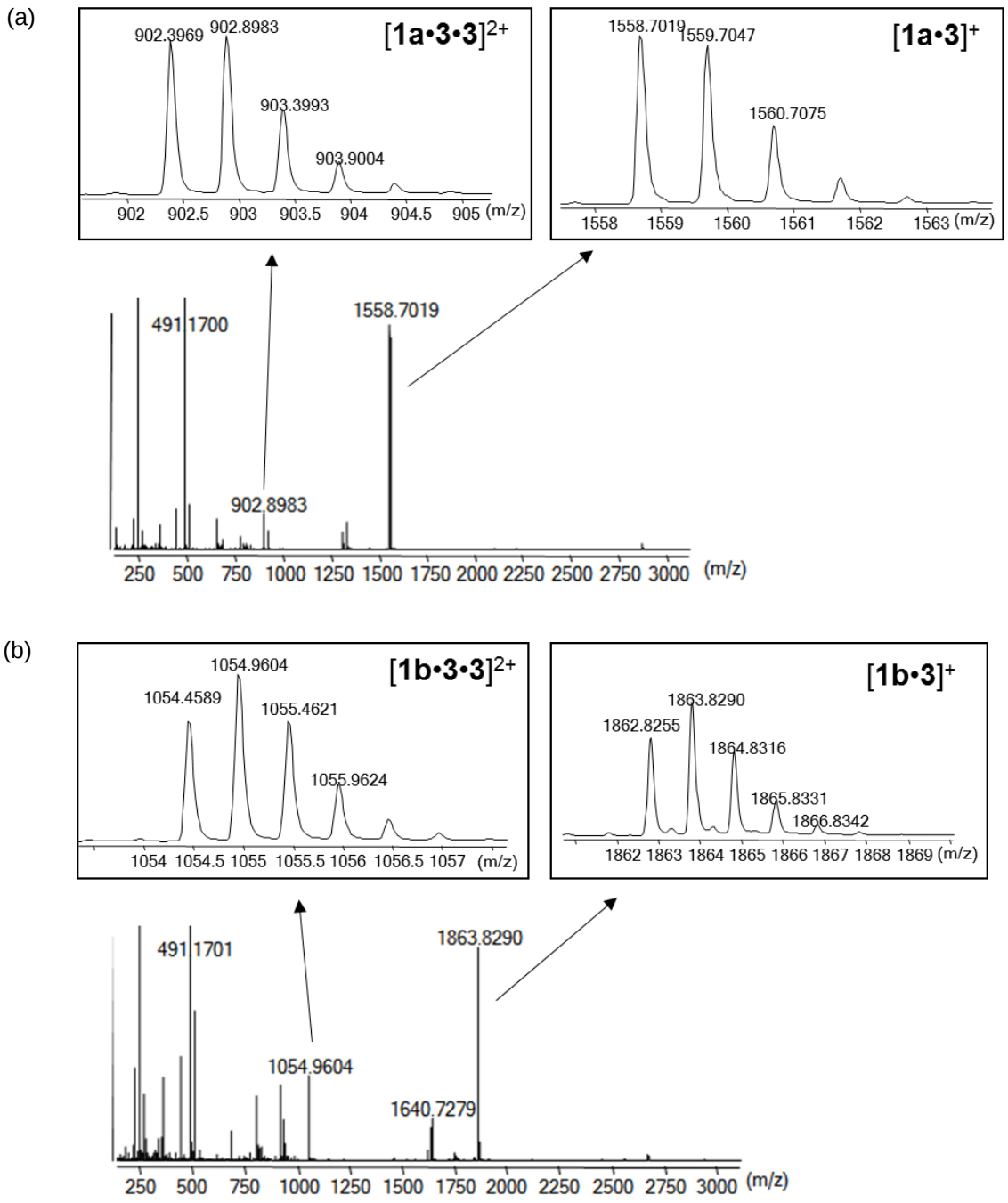


**SI Figure 8**. HRMS spectra of mixtures of (a) **1a**, **3•HFBA** and TFAD, and (b) **1b**, **3•HFBA** and TFAD observed by Accurate Mass LC-TOF (Agilent). Insets are the extended regions indicating $\mathbf{[H•G]^+}$ and $\mathbf{[H•G_2]^{2+}}$.

(a) $^1$H NMR spectrum of the host-guest methyls ($Me_a$ & $Me_b$) and the free host methyl (**1b** Me).

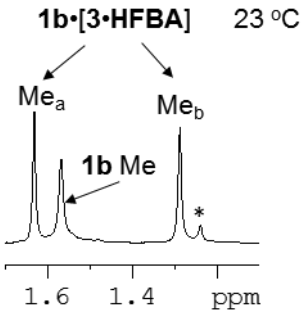


Relative intensity of the corresponding methyl signal was computed by first normalizing the integral and then subtracting the value at $t_m$=0.

(b) Typical dynamic exchange plots for a system exchanging between two states.

Exchange plot from the **1b** methyl to $Me_b$ in **1b•[3•HFBA]**. Solution was prepared from **1b** (4.0 mM in 10%MeCN-$d_3$/$CD_2Cl_2$), **3•HFBA** (2.2 equiv) and TFAD (12 equiv). Under these conditions the host speciates as follows: 61% **1b•[3•HFBA]** and 39% **1b**.

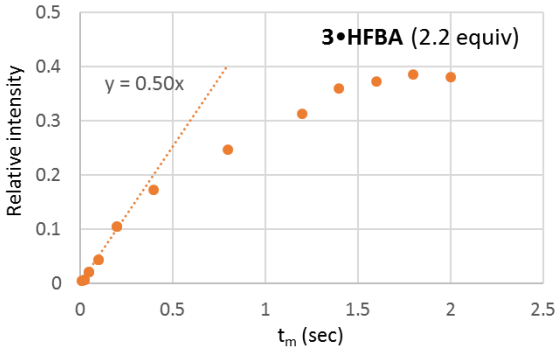


Exchange plot from the **1b** methyl to $Me_b$ in **1b•[3•HFBA]**. Solution was prepared from **1b** (4.0 mM in 10%MeCN-$d_3$/$CD_2Cl_2$), **3•HFBA** (4.3 equiv) and TFAD (12 equiv). Under these conditions the host speciates as follows: 74% **1b•[3•HFBA]** and 26% **1b**.

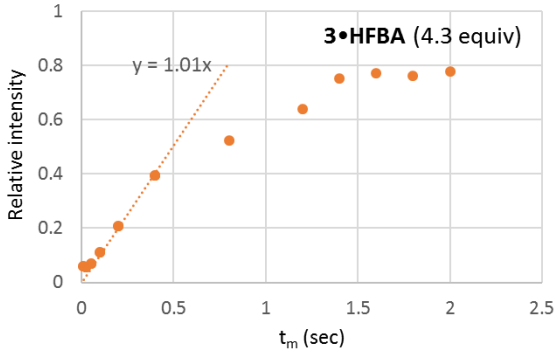


(c) Rates of dynamic exchange of the methyl groups of free host **1b** and the host-guest complex **1b•[3•HFBA]** at room temperature.

| | Rates ($s^{-1}$) of **1b** methyl to **1b•[3•HFBA]** methyls ($Me_a$ &$Me_b$) | | | Rates ($s^{-1}$) of **1b•[3•HFBA]** methyls ($Me_a$ & $Me_b$) to **1b** methyl | | | Rates ($s^{-1}$) between two methyls ($Me_a$ & $Me_b$) of **1b•[3•HFBA]** | | |
|---|---|---|---|---|---|---|---|---|---|
| Guest | **1b** Me to $Me_a$ | **1b** Me to $Me_b$ | Ave | $Me_a$ to **1b** Me | $Me_b$ to **1b** Me | Ave | $Me_a$ to $Me_b$ | $Me_b$ to $Me_a$ | Ave |
| 2.1 eq | 0.56 | 0.50 | 0.53 ±0.036 | 0.48 | 0.51 | 0.49 ±0.018 | 1.00 | 1.03 | 1.02 ±0.024 |
| 4.3 eq. | 1.28 | 1.01 | 1.14 ±0.187 | 0.45 | 0.47 | 0.46 ±0.017 | 1.30 | 1.45 | 1.37 ±0.105 |

**SI Figure 9**. Rates of dynamic exchange for free host **1b** and the host-guest complex **1b•[3•HFBA]** at room temperature. Exchange rates were computed by the relative intensity plots of the relevant methyl signals (eg. (b)) of each species as a function of $t_m$ (mixing time) in a series of 1D EXSY experiments. Due to the limited sample concentrations, 1D EXSY experiments were processed instead of the more time-consuming 2D EXSY experiments. The pulse sequence for the 1D EXSY experiments (90°-$t_1$-90°-$t_m$-90°-$t_2$ pulse sequence with a choice of $t_1$'s) was reported in the following publication (Perrin, C. L.; Engler, R. E. *J. Am. Chem. Soc.* **1997**, *119*, 585-591).

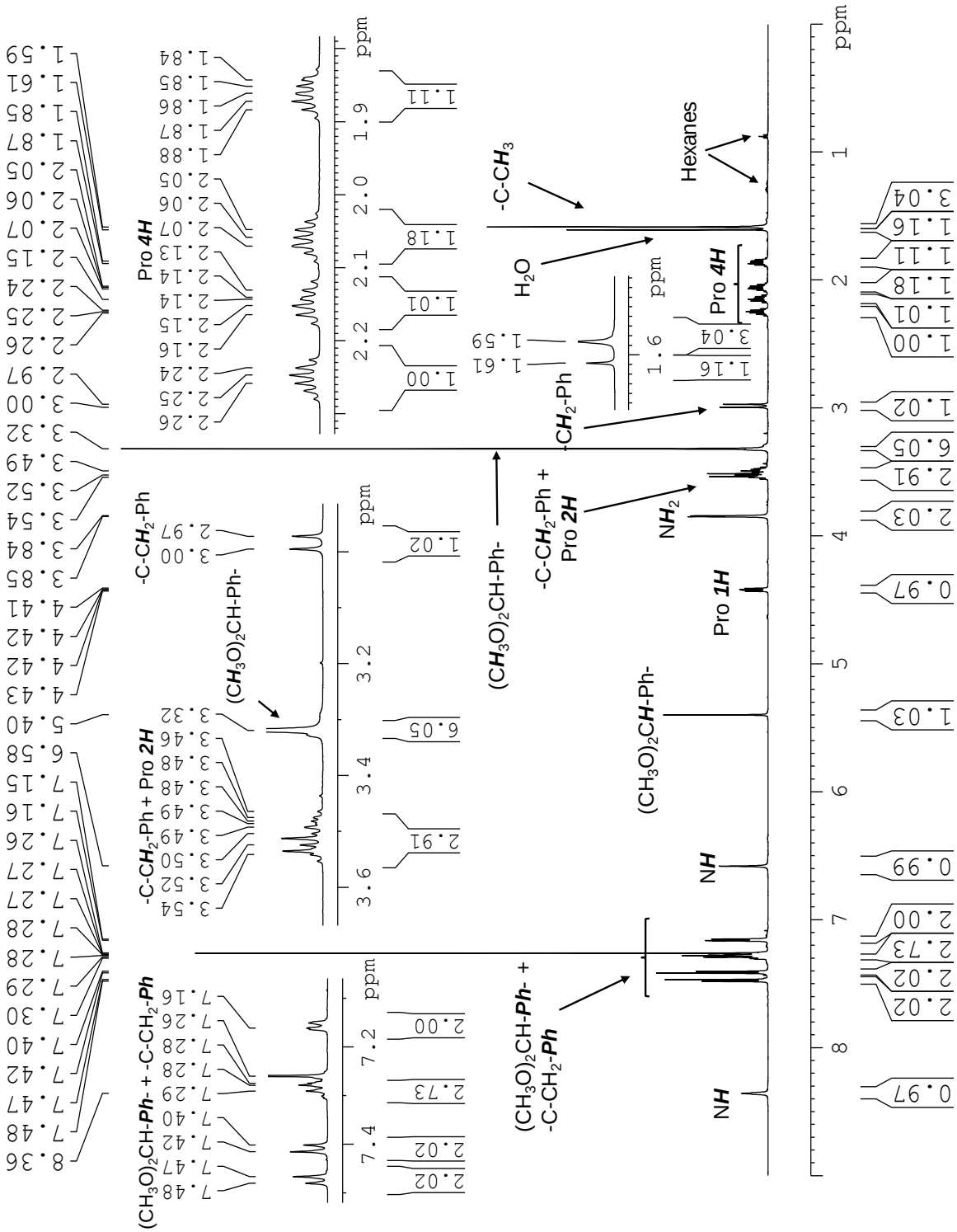


**SI Figure 10.** $^{1}$H NMR spectra of monomer D-Pro-α-Me-L-Phe (600.1 MHz, $CDCl_3$, 23 ºC).

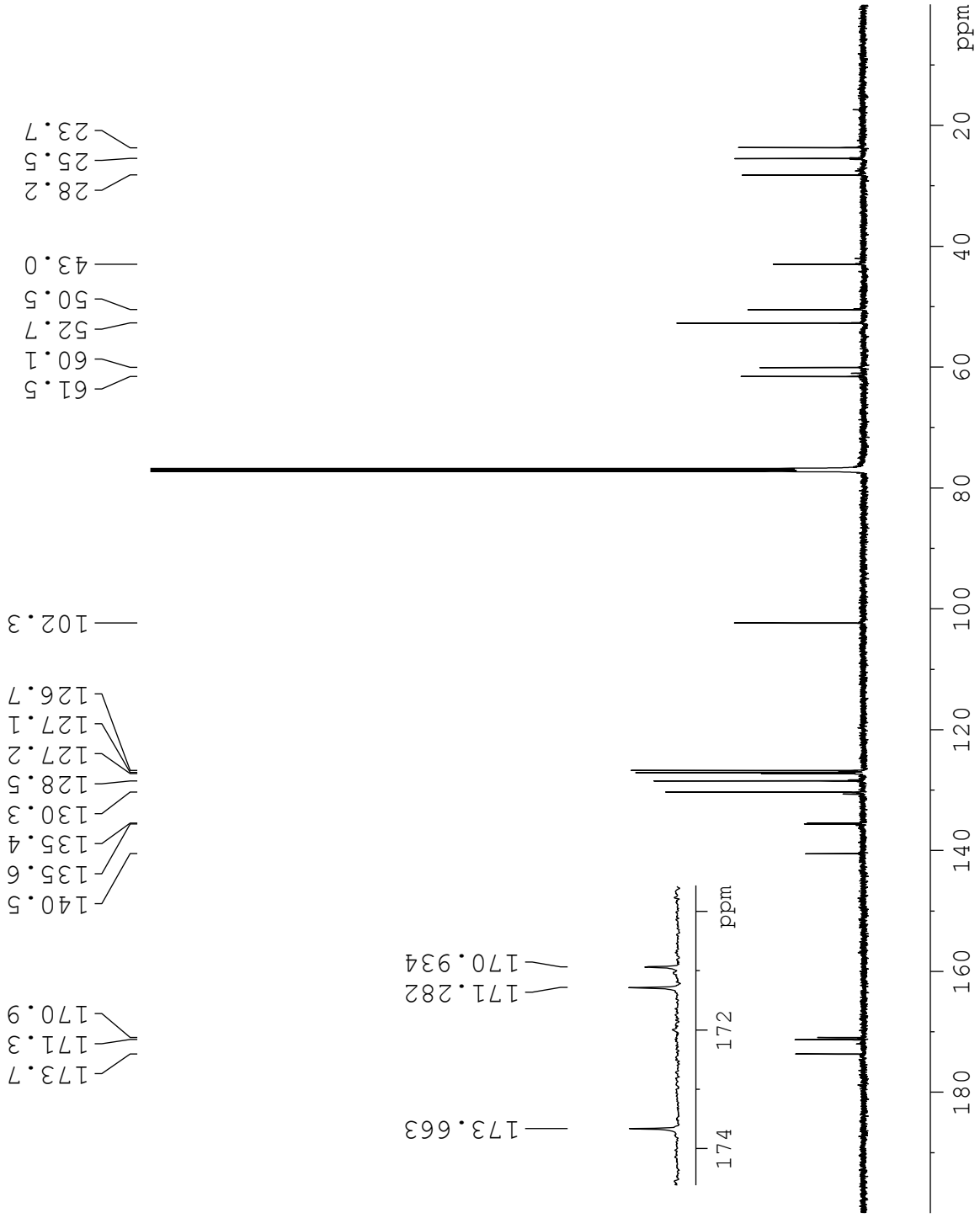


**SI Figure 11.** $^{13}C$ NMR spectra of monomer D-Pro-α-Me-L-Phe (150.9 MHz, $CDCl_3$, 23 ºC).

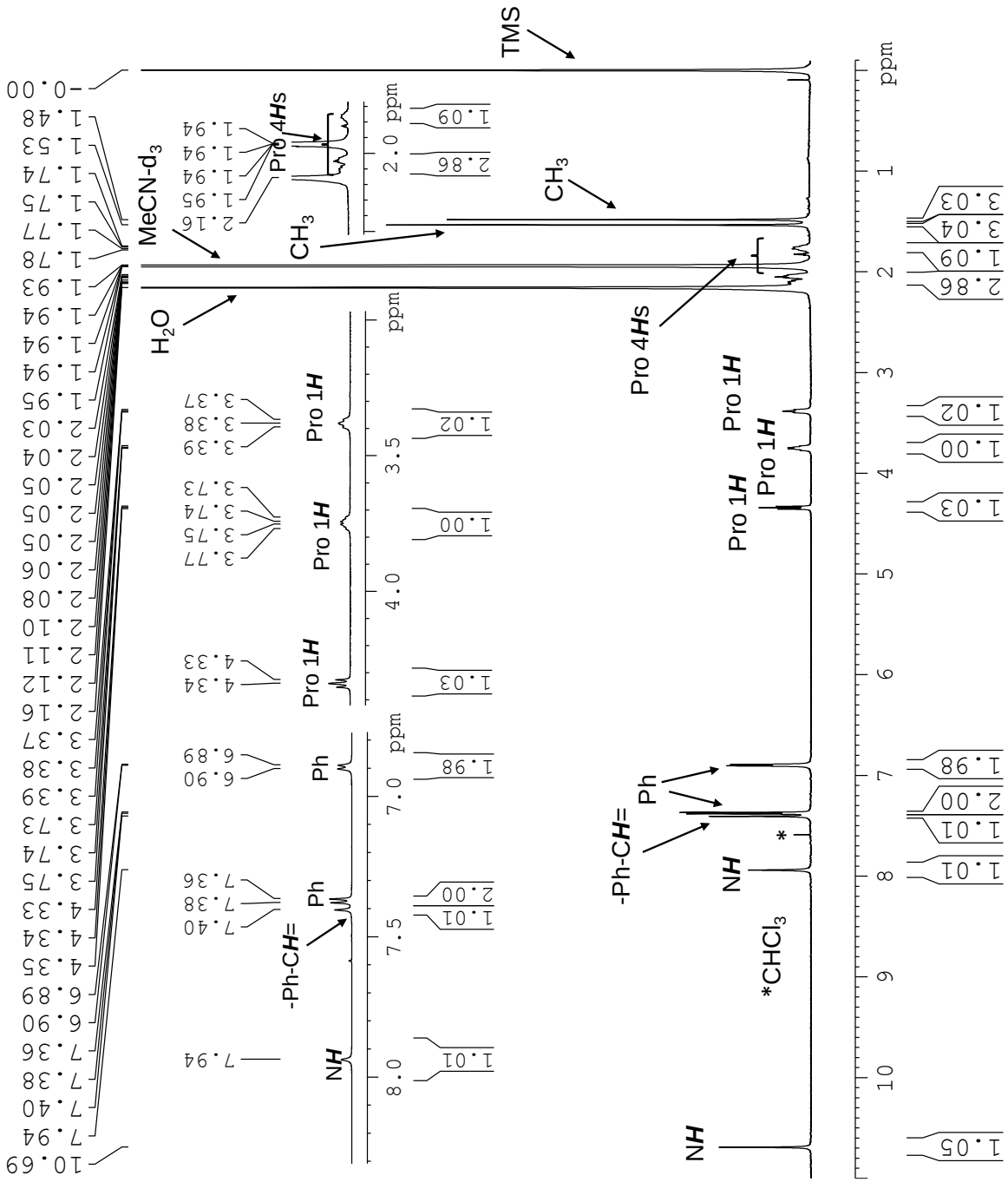


**SI Figure 12.** $^{1}$H NMR spectra of tetramer **1a** (600.1 MHz, MeCN-$d_3$ with TMS, 23 ºC).

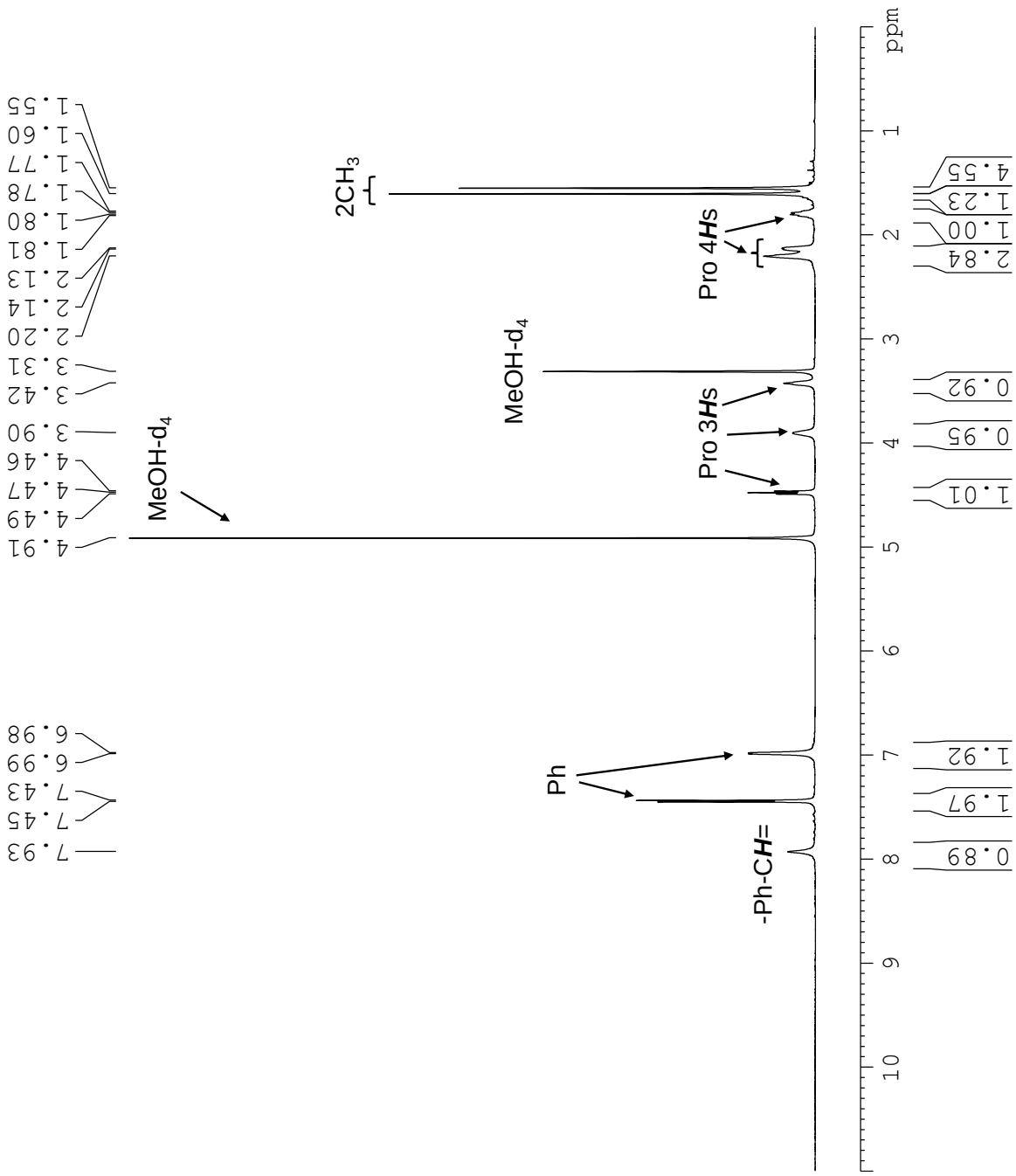


**SI Figure 13.** $^{1}$H NMR spectra of tetramer **1a** (600.1 MHz, MeOH-$d_4$, 23 ºC).

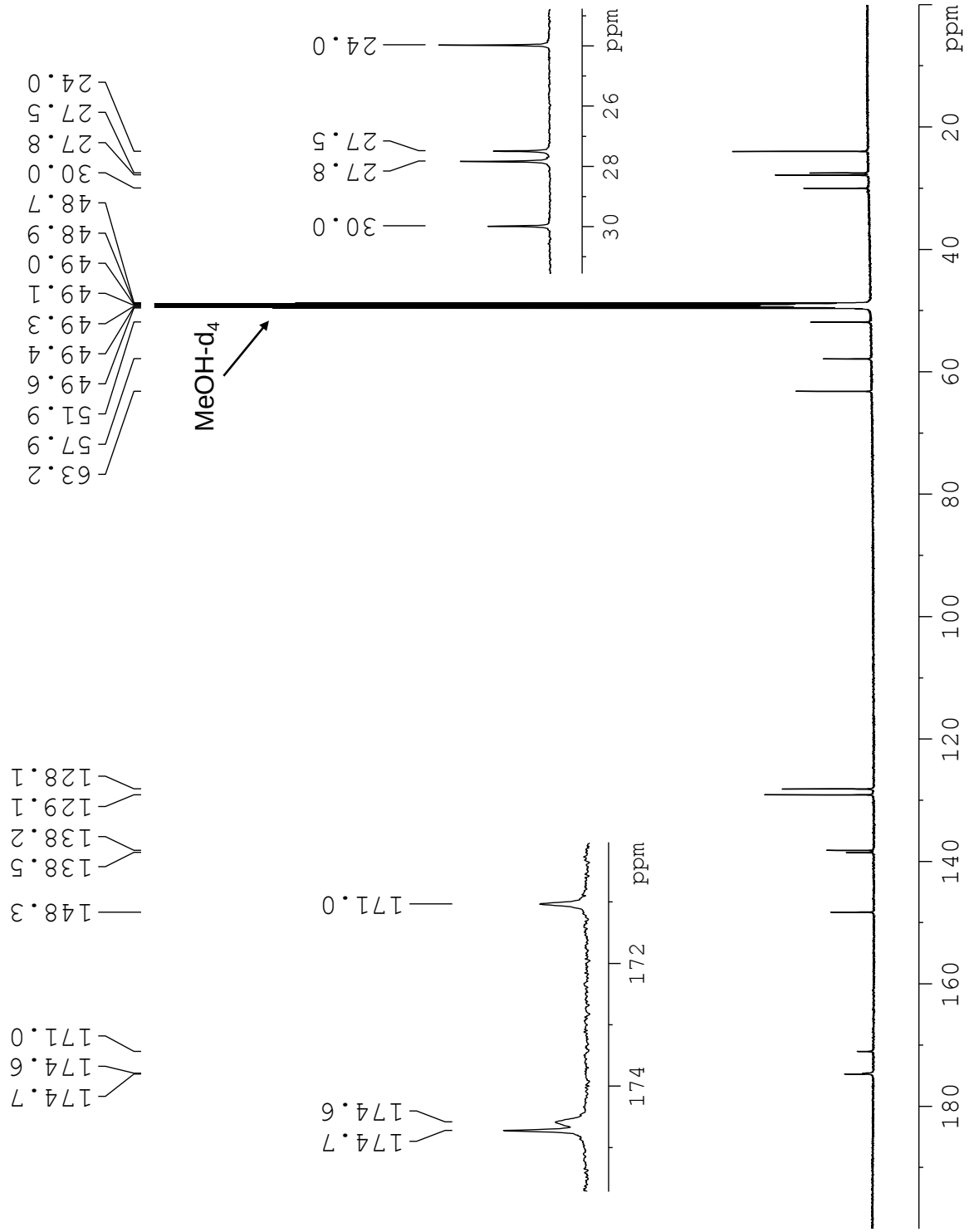


**SI Figure 14.** $^{13}C$ NMR spectra of tetramer **1a** (150.9 MHz, MeOH-$d_4$, 23 ºC).

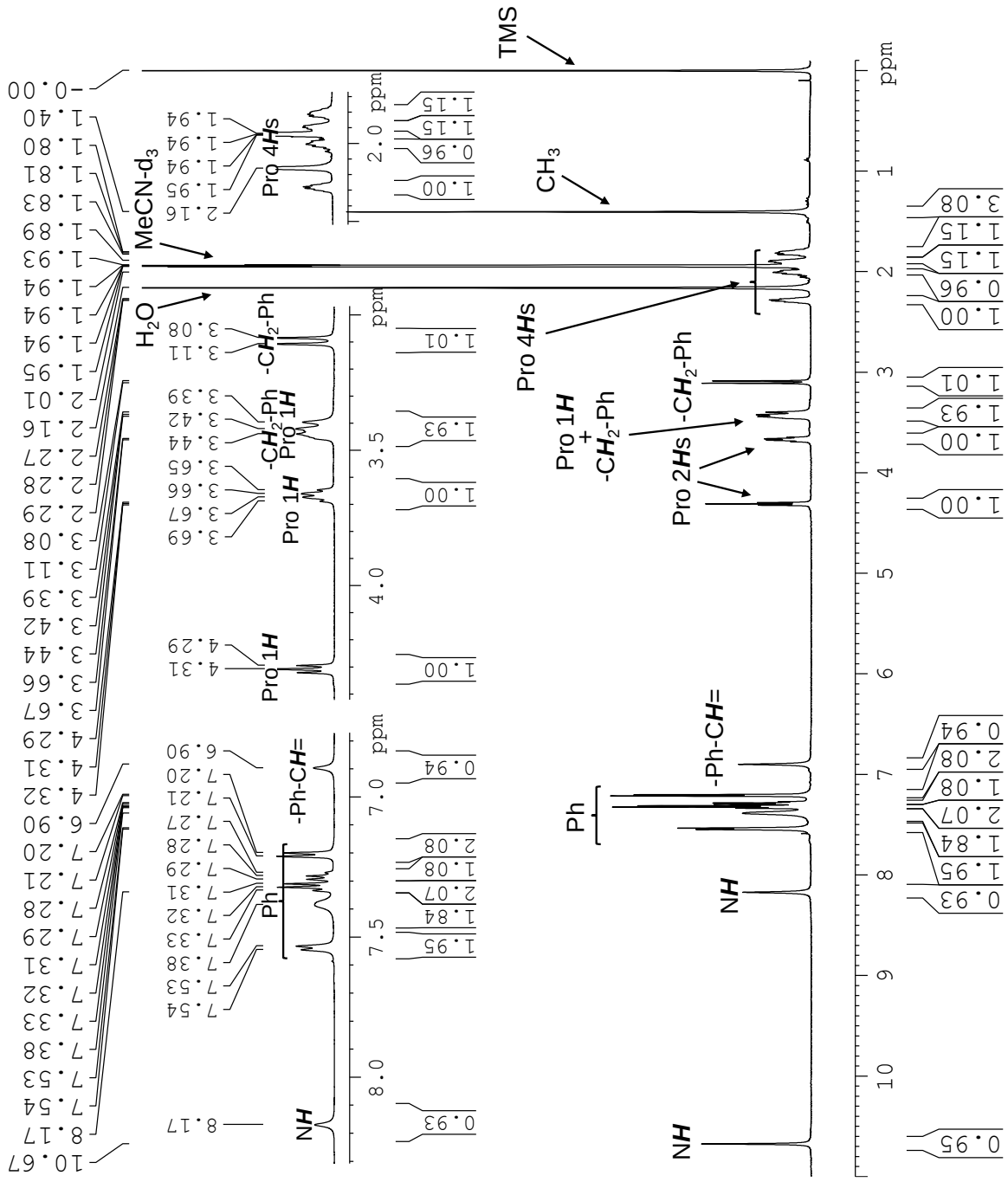


**SI Figure 15.** $^{1}$H NMR spectra of tetramer **1b** (600.1 MHz, MeCN-$d_3$ with TMS, 23 ºC).

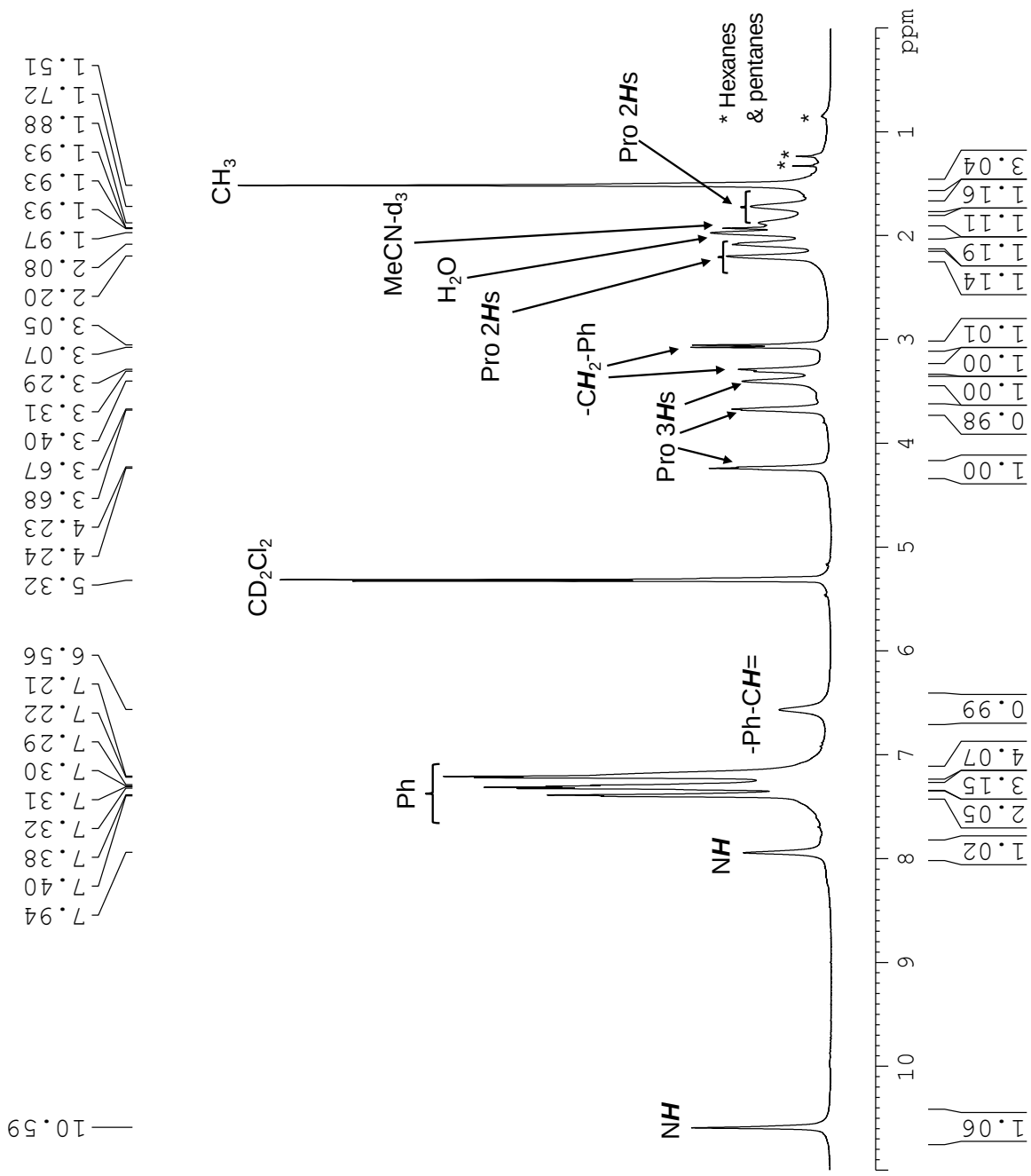


**SI Figure 16.** $^{1}$H NMR spectra of tetramer **1b** (600.1 MHz, 10% MeCN-$d_3$/$CD_2Cl_2$, 23 ºC).

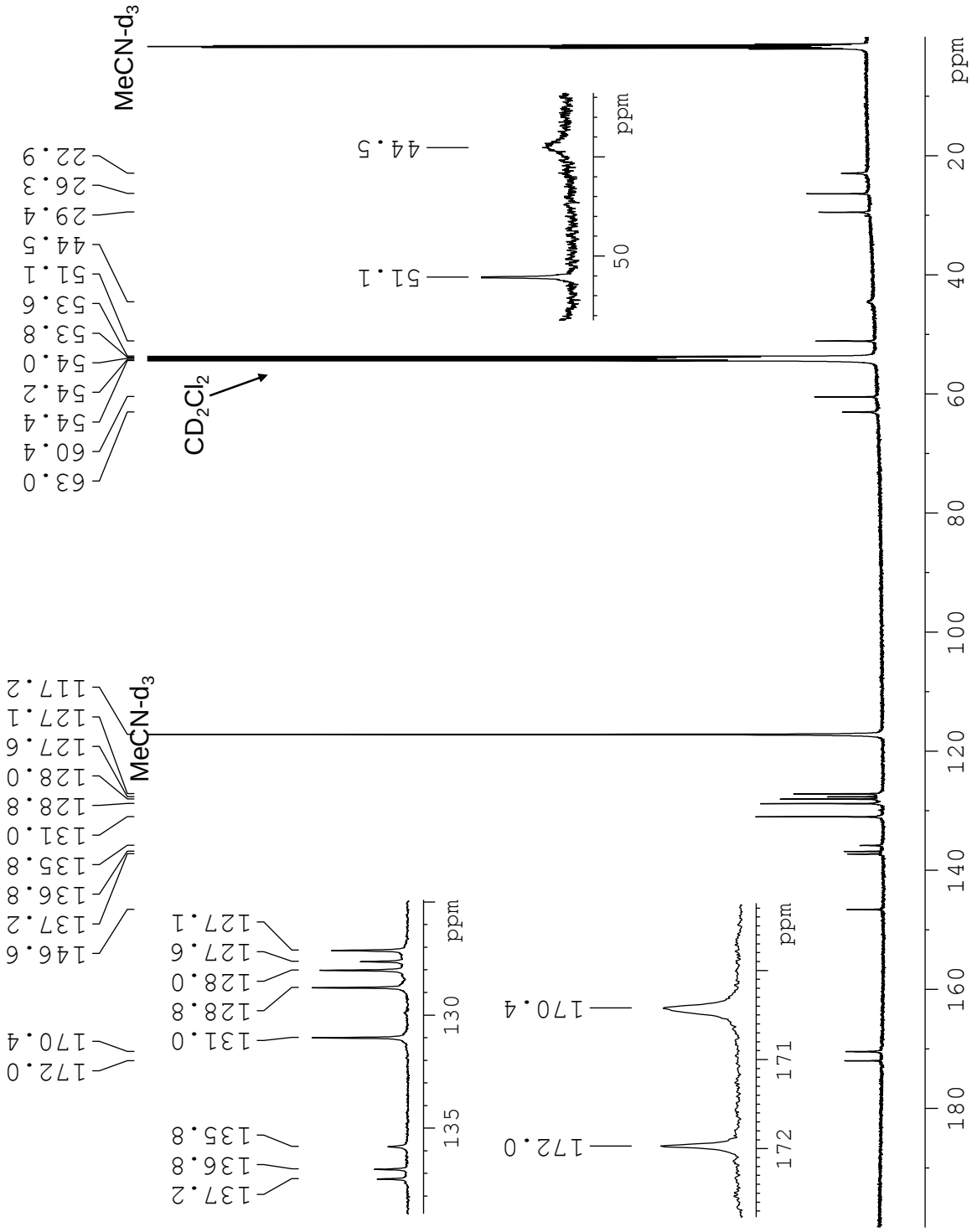


**SI Figure 17.** $^{13}C$ NMR spectra of tetramer **1b** (150.9 MHz, 10% MeCN-$d_3$/$CD_2Cl_2$, 23 ºC).